TABLE 4 Resonance Frequencies F_0 and Gain Measured for Singe-Layered Antennas Realized with Both Plating Processes in Three Bands

Band		Copper	Screen Printing
L	F_0 (GHz)	2.00	1.98
	Gain (dB)	8.5 ± 0.2	7.5 ± 0.2
S	F_0 (GHz)	3.28	3.24
	Gain (dB)	9.0	8.0 ± 0.2
C	F_0 (GHz)	4.6 ± 0.2	4.58
	Gain (dB)	8.2 ± 0.2	7.3 ± 0.2

A. Thermal Shocks. The antennas were subjected to

100 cycles of temperature variation from −30°C to 50°C
100 cycles from −40°C to 85°C
100 cycles from −55°C to 100°C
100 cycles from −65°C to 125°C

During the last cycles (−65°C to +125°C), a breakage appeared in the foam.

B. Damp Heat. The antennas were stored in a steam room at 40°C and 95% relative humidity for 18 days. They were measured before and after this test: A frequency shift of 1% is noticed.

1. CONCLUSION

In this article, two plating processes for polypropylene and foam are described. They were used to realize printed radiating elements of multilayered antennas. Such antennas are compact, wideband (15%), and directive (8–9 dB). Therefore they are of great interest for mobile communication, and with the increasing development of the latter in UHF band, we think that this kind of antenna can have interesting industrial applications.

ACKNOWLEDGMENTS

We would like to thank Y. Leroux and G. Gerard (CNET Lannion) for their assistance in the device fabrication.

REFERENCES

1. G. Kossavias and A. Papiernik, "A Circularly or Linearly Polarized Broadband Microstrip Antenna Operating in L-Band," *Microwave J.*, May 1992, pp. 266–272.
2. A. C. Tarot, A. Sharaiha, C. Terret, Y. Garnier, L. Demeuré, Y. Le Roux, and J. P. Blot, "Low Cost Technology for Printed Antennas," *Proc. JINA*, Nov. 1994, pp. 382–385.
3. L. Demeuré, Y. Garnier, and Y. Le Roux, "Support Métallisé à Base de Mousse Organique. Assemblage d'au Moins 2 de ces Supports et Procédé de Fabrication de ce Support," French Pattern No. 93 14538.
4. L. Demeuré, Y. Garnier, A. C. Tarot, and A. Sharaiha, "Antenne Plane et Procédé de Réalisation d'une Telle Antenne," French Pattern No. 93 12872.
5. S. Assaily, C. Terret, and J. P. Daniel, "Some Results on Broadband Microstrip Antenna with Low Cross-Polar and High Gain, *IEEE Trans. Antennas Propagat.*, Vol. AP-39, No. 3, 1991, pp. 413–415.

Received 12-1-94

Microwave and Optical Technology Letters, 9/1, 5–7

CCC 0895-2477/95

IMPACT OF SPONTANEOUS EMISSION NOISE OF OPTICAL AMPLIFIERS ON THE CHANNEL CAPACITY OF COHERENT SCM SYSTEMS

Jyh-Horng Wu and Jingshown Wu
Department of Electrical Engineering
National Taiwan University

Yang-Han Lee
Department of Electrical Engineering
Tamkang University
Tamsui, Taipei Hsien, Taiwan 25137
Republic of China

KEY TERMS

Optical amplifiers, emission noise, coherent optics, subcarrier mutiplexing

ABSTRACT

Analysis on the channel capacity of a coherent optical subcarrier multiplexing system using optical amplifiers is presented. The performance criterion, that is, the channel transport capability N, is derived in terms of carrier-to-noise ratio, input optical power, and optical amplifier gain. It is found that when the gain of the optical amplifier is large, the spontaneous emission noise limits the number of channels that can be transmitted in this system. As an example, when the gain is well above 20 dB and input optical power is −28 dBm, the maximum value of N is 46. In addition, the optimum phase modulation index is also presented.

I. INTRODUCTION

Multichannel coherent optical-fiber transmission is apparently a very promising technique for future communication services [1]. Especially, efficient multichannel transmission can be achieved with one optical carrier using subcarrier multiplexing (SCM) techniques [2]. SCM networks provide an attractive approach for utilizing the wide bandwidth of single-mode fiber and electro-optic components, while taking advantage of commercially available microwave electronics. In such a system, an optical amplifier is essential for boosting signals to levels needed for suitable reception [3]. Amplification serves to overcome splitting losses associated with distribution fan out as well as coupler, tap, and line losses [4, 5]. On the other hand, for higher optical amplifier gains, the spontaneous emission noise of the amplification process is a serious impairment, so that there is concern about a role for system performance [6]. In this Letter, we investigate the impact of spontaneous emission noise of optical amplifiers on the coherent optical frequency-shift-keying (FSK) SCM systems. The performance criterion, that is, the channel transport capability N, is derived in terms of carrier-to-noise ratio (CNR), input optical power, and optical amplifier gain. It is shown that when the gain of the optical amplifier is large, the spontaneous emission noise imposes a limit on the number of channels that can be transmitted in the system.

II. SYSTEM DESCRIPTION AND ANALYSIS

A. System Description. Figure 1 shows the schematic diagram of a coherent optical SCM system with N channels. The microwave FSK signals are generated by modulating individual voltage-controlled oscillators at distinct subcarrier frequencies, combined with a power combiner, and then fed to the phase modulator. At the receiving end, the optical amplifier used as a preamplifier is employed to boost the optical signal, and the optical filter limits the bandwidth of the

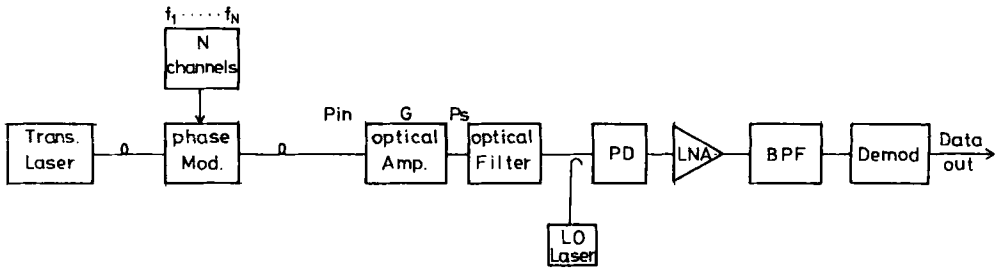

Figure 1 A schematic diagram of coherent optical FSK-SCM systems using optical amplifier

spontaneous emission noise. Then the signal is mixed with the local oscillator (LO) via a 3-dB coupler and detected by a p-i-n photodiode. The output of the photodiode is amplified by a low-noise amplifier (LNA), and the bandpass filter (BPF) is used to select the desired channel. The following is a typical FSK demodulator. In such a structure, the noise components at the output of the BPF consist of shot noise, thermal noise, intermodulation distortion (IMD), signal-spontaneous emission beat noise, and spontaneous-spontaneous emission beat noise. For the sake of simplicity, we use Gaussian approximation. Therefore, the variances of these noises are given as (Table 1 shows the meaning of each parameter and the values of fixed constants [2, 6])

$$\sigma_{sh}^2 = 2eRP_{LO}B, \tag{1}$$

$$\sigma_{th}^2 = \langle i_{th}^2 \rangle B, \tag{2}$$

$$\sigma_{imd}^2 = h_3 k_3(i) R^2 P_{LO} P_S \beta^6/32, \tag{3}$$

$$\sigma_{s-sp}^2 = 4R(P_S + P_{LO})\eta_o e \eta N_{sp}(G-1)B, \tag{4}$$

$$\sigma_{spsp}^2 = 2[\eta\eta_o N_{sp}(G-1)e]^2 B \Delta f_0. \tag{5}$$

The CNR of Channel i at the output of the BPF is given by [6]

$$\mathrm{CNR} = \frac{A\beta^2}{\sigma_{sh}^2 + \sigma_{th}^2 + \sigma_{imd}^2 + \sigma_{spLO}^2 + \sigma_{spsp}^2}, \tag{6}$$

where

$$A = 0.5R^2 P_{LO} P_S \tag{7}$$

and

$$P_S = P_{in}\eta_i G \eta_o. \tag{8}$$

The number of IMD of Channel i, $k_3(i)$, can be expressed as [7]

$$k_3(i) = \frac{i(N-i+1)}{2} + \frac{[(N-3)^2 - 5]}{4}. \tag{9}$$

For such a system, every channel has almost the same performance in our analysis [2]. In the following derivation, we consider CNR of the central channel $[i = (N+1)/2]$, which has the most IMD as the criterion; thus $k_3[(N+1)/2]$ is $(3N^2 - 10N + 9)/8$.

B. Analysis. From (6) and (9), we can get CNR of the central channel as

$$\mathrm{CNR} = \frac{A\beta^2}{\sigma_{sh}^2 + \sigma_{th}^2 + A\beta^6(N^2 - \frac{10}{3}N + 3)/64 + \sigma_{s-sp}^2 + \sigma_{spsp}^2}. \tag{10}$$

TABLE 1 Definition of Symbols Used

Symbol	Definition	Value
N	Channel number	
R	Photodiode responsivity	0.75 A/W
η	Photodiode quantum efficiency	0.6
P_{in}	Input optical power to amplifier	
P_S	Optical power at photodiode	
η_i	Amplifier input coupling loss	4 dB
η_o	Amplifier output coupling loss	4 dB
G	Amplifier gain	
e	Electron charge	$1.6 \cdot 10^{-19}$ C
B	Electrical bandwidth	120 MHz
N_{sp}	Spontaneous emission factor	1
β	Phase modulation index	
P_{LO}	Local oscillator power	−3 dBm
$\langle i_{th}^2 \rangle$	Thermal noise	6.65×10^{-22} A²/Hz
h_3	IMD parameter	$\frac{2}{3}$
k_3	Number of third order IM products	
Δf_0	Bandwidth of the optical filter	4 nm

With simple algebraic manipulation, we obtain

$$N^2 - \frac{10}{3}N + 3 = 64\left(\frac{1}{\mathrm{CNR}\cdot\beta^4} - \frac{\sigma^2}{A\beta^6}\right), \tag{11}$$

where

$$\sigma^2 = \sigma_{sh}^2 + \sigma_{th}^2 + \sigma_{s-sp}^2 + \sigma_{spsp}^2. \tag{12}$$

Note that the left side of (11) is a monotonically increasing function of N when $N > 5/3$, which is the case of practical interest. We can thus maximize N by optimizing β, when P_{in}, G, and CNR are fixed. Differentiating the right-hand side of (11) with respect to β and set to zero, we get

$$\beta_{opt} = \sqrt{\frac{3\sigma^2 \mathrm{CNR}}{2A}}. \tag{13}$$

Therefore, the maximum value of N is

$$N_{max} = \frac{16}{9}\sqrt{3}\cdot\frac{A}{\sigma^2}\cdot\mathrm{CNR}^{-(3/2)} + \frac{5}{3}. \tag{14}$$

C. Discussion. We may make some reasonable approximations to get a further insight into (13) and (14). In general, when the amplifier gain G is large, the signal-spontaneous emission beat noise dominates the noise term [6]. Thus when

$G \gg 1$

$$\beta_{\text{opt}} \approx \sqrt{\frac{12e\eta N_{\text{sp}} B \cdot \text{CNR}}{R\eta_i P_{\text{in}}}} \tag{15}$$

which is proportional to $P_{\text{in}}^{-1/2}$, and

$$N_{\max} \approx \frac{2}{9}\sqrt{3} \cdot \frac{R\eta_i P_{\text{in}}}{e\eta N_{\text{sp}} B} \cdot \text{CNR}^{-(3/2)} + \frac{5}{3}, \tag{16}$$

which is proportional to P_{in}.

III. NUMERICAL EXAMPLE

Consider a FSK-SCM system for the transmission of N channels, and the following parameters are adopted: CNR = 17 dB, R = 0.75 A/W, B = 120 MHz, and N_{sp} = 1. Using (11), we can get the total channel number versus the phase modulation index for some specified CNR, P_{in} and G, as shown in Figure 2. The optimum value of β that maximizes N decreases with increasing input optical power. Note that the curve is relatively sharp near the optimum phase modulation index. That is, the choice of β is of great importance for this system.

Figure 3 shows the total channel number N versus the amplifier gain G for P_{in} = −32 dBm, −30 dBm, and −28 dBm. Without optical amplifier, that is, $\eta_i = \eta_o = G = 1$, N is 9, 14, and 22 for the three different input optical powers. When the optical amplifier is employed, N can be increased to some extent. As predicted by (16), when spontaneous emission noise dominates, N becomes a constant that depends on P_{in} and is independent of G. From Figure 3, it is seen that when G is sufficiently large, N is increased about twofold (i.e., 19, 29, and 46) for the three different input optical powers.

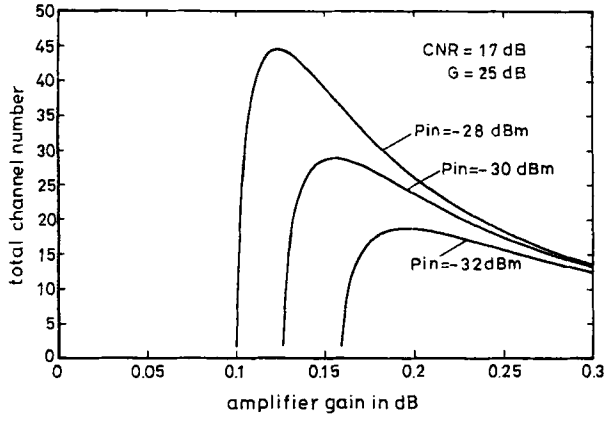

Figure 2 Total channel number versus the phase modulation index for P_{in} = −32 dBm, −30 dBm, −28 dBm. CNR = 17 dB, G = 25 dB.

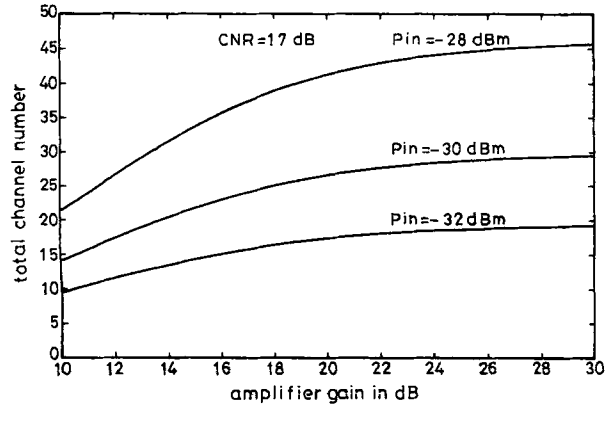

Figure 3 Total channel number versus the optical amplifier gain for P_{in} = −32 dBm, −30 dBm, and −28 dBm. CNR = 17 dB

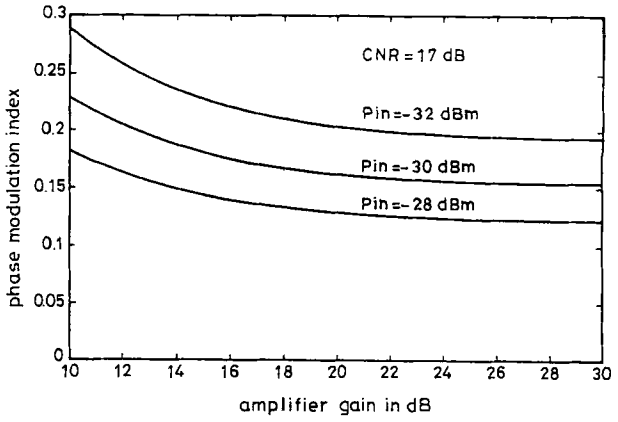

Figure 4 The optimum phase modulation index versus the optical amplifier gain for P_{in} = −32 dBm, −30 dBm, and −28 dBm. CNR = 17 dB

Figure 4 shows the corresponding optimum phase modulation index β versus the amplifier gain G for P_{in} = −32 dBm, −30 dBm, and −28 dBm. As predicted by (15), β decreases with increasing input optical power. When G is large, that is, spontaneous emission noise dominates, β depends only on P_{in} and is independent of G. As shown in Figure 4, for higher amplifier gains, β is 0.193, 0.153, and 0.122 for the three different input optical powers.

IV. CONCLUSION

A general expression of the channel capacity of a coherent optical FSK-SCM system employing optical amplifier is derived in terms of input optical power, carrier-to-noise ratio, and optical amplifier gain. It is found that when local oscillator-spontaneous emission noise dominates, the channel capacity depends only on input optical power and is independent of the gain of optical amplifier, that is, the spontaneous emission noise imposes a limit on the channel transport capability of this system. As an example, when the input optical power is −28 dBm, the limiting value of the total channel number is 46 for CNR = 17 dB.

REFERENCES

1. E. Dietrich, B. Enning, G. Grosskopf, L. Kuller, R. Ludwig, R. Molt, E. Patzak, and H. G. Weber, "Semiconductor Laser Optical Amplifiers for Multichannel Coherent Optical Transmission," *IEEE J. Lightwave Technol.*, Vol. LT-7, No. 12, Dec. 1989, pp. 1941–1955.
2. R. Gross and R. Olshansky, "Multichannel Coherent FSK Experiments Using Subcarrier Multiplexing Techniques," *IEEE J. Lightwave Technol.*, Vol. LT-8, No. 3, March 1990, pp. 406–415.
3. G. J. Foschini and A. M. Saleh, "Overcoming Optical Amplifier Intermodulation Distortion Using Coding in Multichannel Communication Systems," *IEEE Trans. Commun.*, Vol. COM-38, No. 2, Feb. 1990, pp. 187–191.

4. N. A. Olsson, "Lightwave Systems with Optical Amplifiers," *IEEE J. Lightwave Technol.*, Vol. LT-7, No. 7, July 1989, pp. 1071–1082.
5. R. Noe, C. E. Zah, M. Maeda, C. Caneau, S. G. Menocal, R. E. Wanger, and T. P. Lee, "Optical Amplifier with 27 dB Dynamic Range in a Coherent Transmission System," *IEEE Photon. Technol. Lett.*, Vol. PTL-2, No. 2, Feb. 1990, pp. 120–121.
6. R. W. Gross, W. Rideout, R. Olshansky, and G. R. Joyce, "Heterodyne Video Distribution Systems Sharing Transmitter and Local Oscillator Lasers," *IEEE J. Lightwave Technol.*, Vol. LT-9, No. 4, April 1991, pp. 524–529.
7. M. T. Abuelma'atti, "Carrier-to-Intermodulation Performance of Multiple FM/FDM Carriers through a GaAlAs Heterojunction Laser Diode," *IEEE Trans. Commun.*, Vol. COM-33, No, 3, 1985, pp. 246–248.

Received 10-17-94; revised 12-19-94

Microwave and Optical Technology Letters, 9/1, 7–10

CCC 0895-2477/95

REDUCED-THRESHOLD-CURRENT VERTICAL CAVITY SURFACE-EMITTING LASER

M. A. Matin,* T. M. Benson, J. W. Orton, and D. E. Lacklison
Department of Electrical and Electronic Engineering
University of Nottingham
University Park, Nottingham NG7 2RD, United Kingdom

A. F. Jezierski† and C. T. Foxon
Department of Physics
University of Nottingham
University Park, Nottingham NG7 2RD, United Kingdom

J. S. Roberts and T. E. Sale
Department of Electronic and Electrical Engineering
University of Sheffield
PO Box 600
Sheffield SI 4DU, United Kingdom

KEY TERMS

Surface-emitting lasers, threshold current, semiconductor lasers

ABSTRACT

A simple method for reducing the threshold current of vertical cavity surface-emitting lasers (VCSELs) is described. The approach modifies the top surface of the laser into a dome shape by chemical etching. This reduces the reflectance of the top mirror over an approximately annular region, thereby reducing the lasing area compared to the contact area in a controlled manner. A sevenfold reduction in threshold current over equivalent conventional VCSELs is demonstrated for a nonoptimized device that maintains a similar threshold current density. © 1995 John Wiley & Sons, Inc.

1. INTRODUCTION

In recent years much progress has been made in the development of vertical cavity surface-emitting lasers (VCSELs) for applications in communications [1, 2] and addressable arrays [3]. VCSELs also open the door to wider applications such as laser scanning, laser printing, medical imaging, optical memory, visual displays, optical computing, and optical interconnects [4]. In order to be commercially viable, however, VCSELs require high efficiency and low threshold current [5]. This Letter describes a simple method for reducing the threshold current of a VCSEL, by restricting the lasing area in a controlled manner. The method uses standard processing techniques, without recourse to fine scale lithography.

NEW METHOD

Our method involves making a standard VCSEL structure but with a diameter larger than that ultimately required. The top surface of the large device is then modified (here by chemical etching with HF) to produce a mesa with a dome-shaped top, as illustrated in Figure 1. This reduces the reflectance of the top Bragg mirror over an approximately annular region toward the edge of the mesa, while leaving the center region unaffected. The laser lases only in the central region, which can be made much smaller than the overall mesa area. The current is channeled preferentially into the lasing region, so for the same threshold current density the threshold current is correspondingly reduced. A further benefit of the new structure should also be noted; because laser action is confined to a restricted area in the central region of the mesa it is less likely to be degraded by any wall damage resulting from the mesa etching.

FABRICATION

A conventional VCSEL structure was grown by atmospheric-pressure metal-organic vapor-phase epitaxy (MOVPE). The top mirror consists of an epitaxially grown 15-pair GaAs/AlAs quarter-wave reflector with 200-Å-thick $Ga_{0.7}Al_{0.3}As$ layers at each interface for reducing the series resistance. This reflector is p^+ type, 5×10^{18} cm^{-3}, doped with zinc. The bottom mirror consists of a 23-pair AlAs/GaAs quarter-wave reflector with 200-Å-thick $Ga_{0.7}Al_{0.3}As$ layers at each interface and is n type, 1×10^{18} cm^{-3}, doped with silicon. All Al-containing layers include carbon doping from the decomposition of trimethylaluminum, in addition to the zinc and silicon doping. This is a significant contribution to the doping in the p-type AlAs layers. An additional zinc doping spike is included at the stack interfacial layers by virtue of the greater incorporation when growing the intermediate composition, and this helps to further reduce the resistance at the heterointerface. A half-wavelength (0.13-μm-thick) phase-matching capping layer of GaAs p^{++}-doped 1×10^{19} cm^{-3} with zinc is provided. The active region consists of three 85-Å-thick strained $In_{0.22}Ga_{0.78}As$ quantum wells in a 2λ-long undoped GaAs cavity region. Large (70 μm × 70 μm) mesas

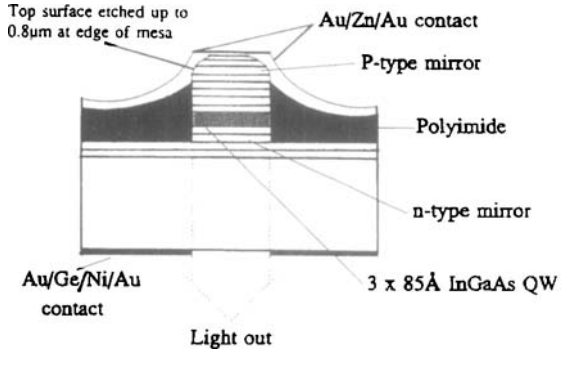

Figure 1 Schematic diagram of a dome-shaped laser structure

*Present address: CEMD, McMaster University, Hamilton, Ontario, Canada L8S 47.
†Present address: Bookham Technology Ltd., Rutherford Appleton Laboratory Chilton, Oxfordshire OX11 OQX, U.K.